PHYSICAL REVIEW D **79,** 034024 (2009)

# Bottomonium dipion transitions

Yu. A. Simonov* and A. I. Veselov†

*ITEP, Moscow, Russia*

(Received 22 June 2008; revised manuscript received 30 September 2008; published 20 February 2009)

Dipion transitions of the subthreshold bottomonium levels $\Upsilon(nS) \to \Upsilon(n'S)\pi\pi$ with $n > n'$, $n = 2, 3, 4$ $n' = 1, 2$ are studied in the framework of the chiral decay Lagrangian, derived earlier. The channels $B\bar{B}$, $B\bar{B}^* + \text{c.c.}$, $B^*\bar{B}^*$ are considered in the intermediate state and realistic wave functions of $\Upsilon(nS)$, $B$ and $B^*$ are used in the overlap matrix elements. Imposing the Adler zero requirement on the transition matrix element, one obtains 2d and 1d dipion spectra in reasonable agreement with experiment.

DOI: 10.1103/PhysRevD.79.034024 PACS numbers: 14.40.Nd, 13.25.Gv

## I. INTRODUCTION

Dipion transitions of heavy quarkonia first discovered in [1] were further experimentally studied in bottomonium $\Upsilon(nS) \to \Upsilon(n'S)\pi\pi$ with $n = 2, 3$, $n' = 1, 2$ by the CLEO Collaboration [2–5], and for $n = 4$, $n' = 1$, 2 by the *BABAR* [6] and Belle Collaborations [7]. Recently a detailed analysis of dipion transitions between states with $n = 1$, 2, 3 was done by the CLEO Collaboration [8]. On the theoretical side the first attempt of explanation of dipion spectra was done in [9–13] using multipole gluon field expansion and PCAC; for a recent development of this model see [14]. However, in this approach the natural explanation can be given only to the $(n, n') = (2, 1)$ dipion spectrum, while other types of spectra with a double peak need additional assumptions, such as the role of final state interaction and $\sigma$ resonance [15–18], exotic $\Upsilon\pi$ resonances [15,19–21], coupled channel effects [22,23], relativistic corrections [24], and $S - D$ mixing [25]. The role of the constant term was studied in [26], for a recent development see [27,28]. In the present paper we are using the formalism of field correlators [29] and the chiral decay Lagrangian [30] developed for the dipion transitions in [31,32]. In this formalism the dipion transition proceeds via $B\bar{B}$, $B\bar{B}^*$, etc. intermediate states and the total amplitude consists of two terms: $\mathcal{M} = a - b$, where $a$ refers to the subsequent one-pion emission at each vertex of the type $\Upsilon \to B\bar{B}$, while $b$ refers to the sequence of zero-pion and two-pion vertices (see Fig. 1). The crucial point for the calculation is the knowledge of the realistic wave functions of all participants. In [31,32] the simplest simple hadronic oscillator (SHO) form was used, fitted to the realistic rms of a given state. In the present paper we are using the realistic wave functions of $\Upsilon(nS)$, $B$ and $B^*$ mesons, calculated in [33] and being in good agreement with spectra and decay constants. To simplify calculations of the overlap matrix elements we are expanding realistic wave functions in series of SHO functions and check accuracy of expansion. Another improvement over results of [31,32] is that we also consider transitions $(n, n') = (4, 1), (4, 2)$ and compare them with experiment [6,7]. On a more fundamental level we are considering not only spectra, but also absolute values of widths both for dipion and for pionless decays of the type $\Upsilon(nS) \to B\bar{B}, B\bar{B}^* + \text{c.c.}, B^*\bar{B}^*$. The detailed analysis, made in the paper, reveals that pionic and pionless decays are governed by distinct vertices, the first one is given by the chiral decay Lagrangian (CDL) [30], while the second one by the relativistic decay Lagrangian (RDL), being in some sense the relativistic generalization of the $^3P_0$ model Lagrangian. Correspondingly we introduce two reasonable physical scales, $M_{\text{br}} \approx f_\pi \approx 0.1$ GeV and $M_\omega \approx 2\omega$, where $\omega$ is the average energy of a light quark in the heavy-light meson ($B$ meson), $\omega \approx 0.5$ GeV. The resulting expressions are otherwise parameter-free and allow us to predict the $\pi\pi$ spectrum in all transitions considered. As was already observed in [31,32], the form of the spectrum is defined by the only real parameter $\eta$, which was calculated in our approach with the account of the Adler zero requirement (this requirement serves as a kind of renormalization condition on amplitudes $a$, $b$). We shall use below the values of Adler zero improved (AZI) $\eta = \eta_{\text{AZI}}$, obtained in [31,32] and predict the $\pi\pi$ spectrum as a function of total $\pi\pi$ mass $M_{\pi\pi} \equiv q$ and angle $\theta$ of $\pi^+$ with respect to the initial $\Upsilon$ direction, making also comparison to experiment. The plan of the paper is as follows. In Sec. II general equations for dipion and pionless amplitudes are given, taken from [31,32], however modified as compared to [31,32] due to

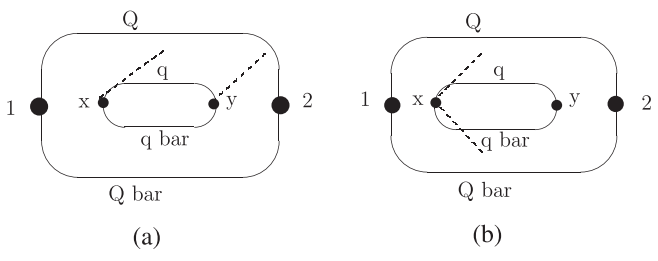


FIG. 1. Diagrams for pion emission from the internal light quark loop. Subsequent one-pion emission (a) and two-pion emission (b).

*simonov@itep.ru
†veselov@itep.ru

 

appearance of two mass parameters $M_{\rm br}$, $M_w$ instead of one, $M_{\rm br}$ in [31]. We also make a correction to Eqs. (53, 55) of [31], valid for equal mass case, to make it suitable for the realistic case.[1] In Sec. III we describe the calculation of overlap matrix elements and expansion of realistic wave functions. In Sec. IV the AZI procedure is exploited for matrix elements, and we show results of calculations for matrix elements and spectra. In Sec. V our results are discussed in comparison with experiment. The last short section is devoted to conclusions and perspectives.

## II. THE BOTTOMONIUM DECAY AMPLITUDES

We start with the definition of Lagrangians for the light $q\bar{q}$ pair creation. As was derived in [30], the CDL has the form (cf. Eq. (39) in [31]) in Euclidean space-time

$$\mathcal{L}_{\rm CDL} = -i\int d^4x\,\bar{\psi}(x)M_{\rm br}\hat{U}(x)\psi(x) \tag{1}$$

where $\hat{U}(x)$ is the Nambu-Goldstone (NG) matrix

$$\hat{U} = \exp\left(i\gamma_5\frac{\varphi_a\lambda_a}{f_\pi}\right), \qquad \varphi_a\lambda_a = \sqrt{2}\begin{pmatrix} \frac{\eta}{\sqrt{6}}+\frac{\pi^o}{\sqrt{2}}, & \pi^+, & K^+ \\ \pi^-, & \frac{\eta}{\sqrt{6}}-\frac{\pi^o}{\sqrt{2}}, & K^0 \\ K^-, & \bar{K}^0, & -\frac{2\eta}{\sqrt{6}} \end{pmatrix}, \tag{2}$$

and $f_\pi = 93$ MeV. The Lagrangian (1) describes the $q\bar{q}$ pair creation with (or without) NG meson emission, and as will be shown below, $M_{\rm br} \approx f_\pi$.

One can recognize in (1) the scalar mass parameter $M_{\rm br}$ violating chiral symmetry due to scalar confinement, as shown in [30]. To the lowest order in the pion field this Lagrangian coincides with that of Weinberg, Manohar, and Georgi (see [30,34] for discussion and applications).

Another type of the $q\bar{q}$ pair creation occurs in the so-called time-turning trajectories (ttt) of a light quark at the boundary of the Wilson loop, when confinement ensures area law of the loop. In this case one can introduce an effective Lagrangian—the relativistic decay Lagrangian (RDL) of the form

$$\mathcal{L}_{\rm RDL} = -i\int d^4x\,\bar{\psi}(x)M_\omega\psi(x). \tag{3}$$

This Lagrangian is actually a substitute of the diagram with a light quark loop, i.e., the diagram of Fig. 1(b) without the right dot. Physically the confining film between the outer and inner loop in Fig. 1(b) deflects the quark trajectory, making it finally the time-turning trajectory, and the cumulative effect of ttt is described phenomenologically by the Lagrangian (3). Note, that as shown in Eqs. (33–38) of [34], the sum of the diagrams of Figs. 1(a) and 1(b) (without the right dot, i.e., with ttt) satisfies conditions of spontaneous symmetry breaking, which implies the Alder zero requirement (AZR). Therefore we impose the AZR on the total amplitude, obtained from (1) and (3). As will be seen the total amplitude satisfying the AZR with $M_\omega$ taken from the decay $\Upsilon(4S) \to B\bar{B}$ describes well the spectra of $\Upsilon(nS) \to \Upsilon(n'S)\pi\pi$. Here $M_\omega$ will be shown to be of the order of $2\omega$, where $\omega$ is the average energy of the light quark in the $B$ meson, $\omega \approx 0.5$ GeV (see Appendix 1 of [31] for exact values and discussion). Note, that $M_\omega \gg M_{\rm br}$, and for pionless decays one can neglect $\mathcal{L}_{\rm CDL}$ as compared to $\mathcal{L}_{\rm RDL}$. We shall use the strong decay formalism developed in [31] and write the amplitude $w_{nm}$ for the bottomonium transition from the state $n$ to the state $m$ with or without additional NG mesons, (cf. Eq. (48) of [31])

$$w_{nm}(E) = \gamma\int\frac{d^3\mathbf{p}}{(2\pi)^3}\sum_{n_2,n_3}\frac{J_{nn_2n_3}J^+_{mn_2n_3}}{E-E_{n_2n_3}(\mathbf{p})} \tag{4}$$

where $\gamma = \frac{M^2}{N_c}$, $M$ is $M_{\rm br}$ or $M_\omega$ depending on pion emission and $J_{nn_2n_3}$ is the overlap matrix element of the $n$-th state of $\Upsilon$ and $n_2$, $n_3$ states of $B\bar{B}$ or $B\bar{B}^*$ etc. For pionless decay one has

$$J_{nn_2n_3}(\mathbf{p}) = \int\bar{y}_{123}\frac{d^3\mathbf{q}}{(2\pi)^3}\tilde{\Psi}_n(c\mathbf{p}+q)\tilde{\psi}_{n_2}(\mathbf{q})\tilde{\psi}_{n_3}(\mathbf{q}). \tag{5}$$

Here $c = \frac{\Omega}{\Omega+\omega} \approx 1$ ($\Omega$ is the energy of the heavy quark in the $B$ meson, $\Omega \approx 4.83$ GeV) and $\bar{y}_{123}$ is the ratio of Dirac traces, $\bar{y}_{123} = \frac{\bar{Z}}{\sqrt{\prod_{i=1}^3\bar{Z}_i}}$, where the projection operators $\bar{Z}_i$ are defined in [31] and are of the order of 1, so that for $\Upsilon(n) \to B\bar{B}$ the value of $\bar{y}_{123}$ reduces to the Dirac trace of the decay matrix element, e.g., for $\Upsilon(nS) \to B\bar{B}$ one has

$$\bar{y}_{123} \cong \bar{Z} = \mathrm{tr}\left(\gamma_i\frac{S^+_Q}{2\Omega}\gamma_5\frac{S^-_{\bar{q}}}{2\omega}\frac{S^+_q}{2\omega}\gamma_5\frac{S^-_{\bar{Q}}}{2\Omega}\right) \tag{6}$$

with $S^\pm_Q = (m_Q \pm \Omega\gamma_4 \mp ip^Q_i\gamma_i)$, $S^\pm_q = m_q \pm \omega\gamma_4 \mp ip^q_i\gamma_i$.

In Appendix 1 of [31] and Appendix A of the present work details of the calculation of $\bar{Z}_i$ are given.

As a result one obtains for $\bar{y}_{123}$

$$\bar{y}_{123} \approx \bar{Z} = \frac{im_Q}{2\Omega^2\omega}\left[q_i(2\Omega+\omega) - p_i\frac{\omega\Omega}{\omega+\Omega}\right] \approx \frac{i}{\omega}\left(q_i - \frac{p_i\omega}{2(\omega+\Omega)}\right). \tag{7}$$

For the one-pion emission at the decay vertex one has instead

[1]The authors are grateful to Yu. S. Kalashnikova for pointing this fact out to us.

$$J^{(1)}_{nn_2n_3}(\mathbf{p},\mathbf{k}) = \int \bar{y}^{(\pi)}_{123}\frac{d^3\mathbf{q}}{(2\pi)^3}\tilde{\Psi}_n\left(c\mathbf{p}-\frac{\mathbf{k}}{2}+\mathbf{q}\right) \times \tilde{\psi}_{n_2}(\mathbf{q})\tilde{\psi}_{n_3}(\mathbf{q}-\mathbf{k}). \quad (8)$$

Here $\bar{y}^{(\pi)}_{123}$ has the same origin as $\bar{y}_{123}$, but accounts for one-pion emission at the vertex $\Upsilon(n)\to(B\bar{B}^*+\text{c.c.})\pi$,

$$\bar{y}^{(\pi)}_{123} = i\delta_{ik}\frac{m_Q^2+\Omega^2}{2\Omega^2}\frac{1}{\sqrt{2\omega_\pi V_3}f_\pi}\approx\frac{i\delta_{ik}}{\sqrt{2\omega_\pi V_3}f_\pi}. \quad (9)$$

Here $V_3$ is the 3d volume, which cancels in final expressions. Finally, expanding the factor $\hat{U}$ in (2) to the second order, one obtains the overlap matrix element for the double pion emission vertex,

$$J^{(2)}_{nn_2n_3}(\mathbf{p},\mathbf{k}_1,\mathbf{k}_2) = \int \bar{y}^{(\pi\pi)}_{123}\frac{d^3\mathbf{q}}{(2\pi)^3}\tilde{\Psi}_n\left(c\mathbf{p}-\frac{\mathbf{K}}{2}+\mathbf{q}\right) \times \tilde{\psi}_{n_2}(\mathbf{q})\tilde{\psi}_{n_3}(\mathbf{q}-\mathbf{K}). \quad (10)$$

Here $\mathbf{K}$ denotes the sum of pion momenta, $\mathbf{K}=\mathbf{k}_1+\mathbf{k}_2$, and with $\boldsymbol{\pi}$ being the isospin vector for pions $\bar{y}^{(\pi\pi)}_{123}$ is

$$\bar{y}^{(\pi\pi)}_{123} = \frac{i\boldsymbol{\pi}_1\boldsymbol{\pi}_2}{f_\pi^2}\frac{\bar{y}_{123}}{[2\omega_\pi(k_1)V_3 2\omega_\pi(k_2)V_3]^{1/2}}. \quad (11)$$

Having defined all overlap matrix elements in $w_{nm}(E)$, Eq. (4), one can now express total amplitudes for processes with or without pion emission. The width of $\Upsilon(nS)$ due to the channel $B\bar{B}$ is given by the equation

$$\Gamma_n = \gamma_\omega\frac{p_{BB}\tilde{M}_{BB}}{4\pi^2}\int d\Omega_p|J_{nn_2n_3}(\mathbf{p})|^2, \qquad \gamma_\omega=\frac{M_\omega^2}{N_c}. \quad (12)$$

The dipion emission amplitude consists of two terms:

$$w^{(\pi\pi)}_{nm}(E) = \gamma\Bigg\{\sum_k\int\frac{d^3p}{(2\pi)^3}\frac{J^{(1)}_{nn_2n_3}(\mathbf{p},\mathbf{k}_1)J^{*(1)}_{mn_2n_3}(\mathbf{p},\mathbf{k}_2)}{E-E_{n_2n_3}(\mathbf{p})-E_\pi(\mathbf{k}_1)} + (1\leftrightarrow 2) - \sum_{n_2'n_3'}\int\frac{d^3p}{(2\pi)^3}\frac{J^{(2)}_{nn_2'n_3'}(\mathbf{p},\mathbf{k}_1,\mathbf{k}_2)J^*_{mn_2'n_3'}(\mathbf{p})}{E-E_{n_2'n_3'}(\mathbf{p})-E(\mathbf{k}_1,\mathbf{k}_2)} - \sum_{k''}\int\frac{d^3p}{(2\pi)^3}\frac{J_{nn_2''n_3''}(\mathbf{p})J^{(2)*}_{mn_2''n_3''}(\mathbf{p},\mathbf{k}_1,\mathbf{k}_2)}{E-E_{n_2''n_3''}(\mathbf{p})}\Bigg\}. \quad (13)$$

The probability of the process $\Upsilon(n)\to\Upsilon(n')\pi\pi$ is obtained from $w^{(\pi\pi)}_{nn'}$ by standard rules

$$dw((n)\to(n')\pi\pi) = |w^{(\pi\pi)}_{nn'}(E)|^2\frac{V_3d^3\mathbf{k}_1}{(2\pi)^3}\frac{V_3d^3\mathbf{k}_2}{(2\pi)^3} \times 2\pi\delta(E(\mathbf{k}_1,\mathbf{k}_2)+E_{n'}-E_n) \quad (14)$$

and the dipion decay width is

$$\Gamma^{(nn')}_{\pi\pi} = \int dw((n)\to(n')\pi\pi) = \int d\Phi|\mathcal{M}|^2 \quad (15)$$

where $d\Phi$ is the phase space factor

$$d\Phi = \frac{1}{32\pi^3N_c^2}\frac{(M^2+(M')^2-q^2)(M+M')}{4M^3} \times\sqrt{(\Delta M)^2-q^2}\sqrt{q^2-4m_\pi^2}dqd\cos\theta \quad (16)$$

with the notations

$$M\equiv M(\Upsilon(n)), \qquad M'\equiv M(\Upsilon(n')), \qquad \Delta M\equiv M-M', \qquad q^2\equiv M^2_{\pi\pi}=(k_1+k_2)^2=(\omega_1+\omega_2)^2-\mathbf{K}^2. \quad (17)$$

The amplitude $\mathcal{M}$ can be written accordingly to (13) as

$$\mathcal{M} = \left(\frac{M_{\text{br}}}{f_\pi}\right)^2\bar{\mathcal{M}}_1-\frac{M_{\text{br}}M_\omega}{f_\pi^2}\bar{\mathcal{M}}_2. \quad (18)$$

At this point we still do not impose on $\mathcal{M}$ the Adler zero requirement.

## III. CALCULATION OF MATRIX ELEMENTS

For the wave function we use the solution of the relativistic Hamiltonian, described in [33], (for a review see the last reference in [29]), where the only input parameters are current quark masses, string tension and $\alpha_s$. As a result one obtains the bottomonium spectrum with accuracy of the order of 10 MeV and a good agreement with experimental lepton widths (see Table 3 in [31]). In what follows we call this function "the realistic wave function," meaning that it is among the best existing ones, but the point-by-point accuracy of it is not actually known.

In this section we describe the method of calculation of $\bar{\mathcal{M}}_1$, $\bar{\mathcal{M}}_2$ based on the expansion of the wave function in the full set of oscillator functions. This allows us to do integrals in the overlap matrix elements $J$, $J^{(1)}$, $J^{(2)}$ analytically, while the specifics of wave functions are represented by the sequence of numbers –coefficients in the expansion, found by the "chi squared" procedure, namely, for any radial excited state wave function found in [33] we write

$$\Psi(nS,r) = \sum_{k=1}^{k_{\max}}c_k^{(n)}\varphi_k(\beta r) \quad (19)$$

where $\varphi_k(\beta r)$ is given in Appendix A, and oscillator parameter $\beta$ as well as coefficients $c_k^{(n)}$ are obtained minimizing $\chi^2$. The quality of approximations for different

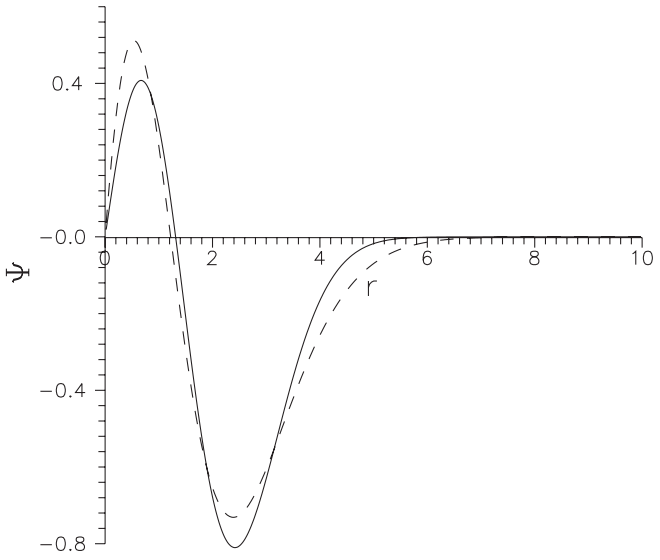


FIG. 2. Realistic wave function of $\Upsilon(2S)$ from [33] (dashed line) and the series of oscillator functions (19) with $k_{\max} = 2$.

$k_{\max}$ can be seen from Figs. 2 and 3. We also compare realistic $B$ meson wave functions computed in [33] with the one-term representation (19) in Fig. 4. (Note, that the $B^*$ wave function is the same as for the $B$ meson in the first approximation used below). Hence, keeping $k = 1$ for $B$, $B^*$ mesons, the simple overlap matrix element (5) without $\bar{y}_{123}$ is

$$J^{(0)}_{n,11}(\mathbf{p}) = \int \frac{d^3\mathbf{q}}{(2\pi)^3} \sum_{k=1}^{N_{\max}} c_k^{(n)} \varphi_k(\beta_1, \mathbf{q} + c\mathbf{p}) \varphi_1^2(\beta_2, \mathbf{q}) = e^{-(\mathbf{p}^2/\Delta)} I_{n,11}(\mathbf{p}) \tag{20}$$

where $\Delta = 2\beta_1^2 + \beta_2^2$, and $I_{n,11}(\mathbf{p})$ is a polynomial in powers of $\mathbf{p}^2$, given in Appendix A.

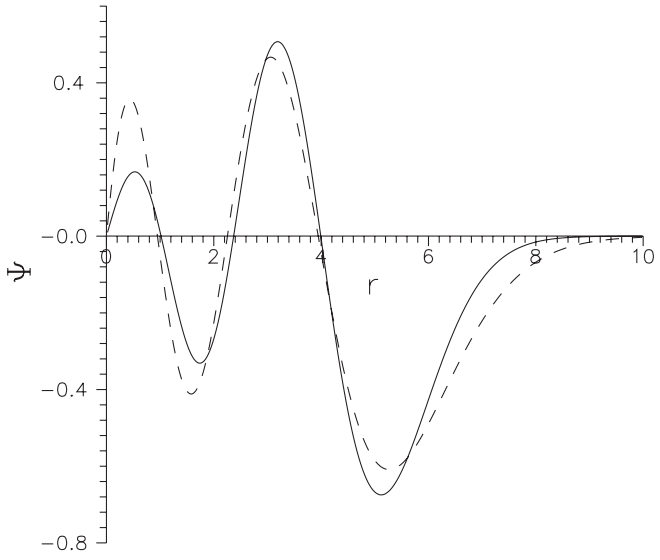


FIG. 3. The same as in Fig. 2, but for $\Upsilon(4S)$ and $k_{\max} = 4$.

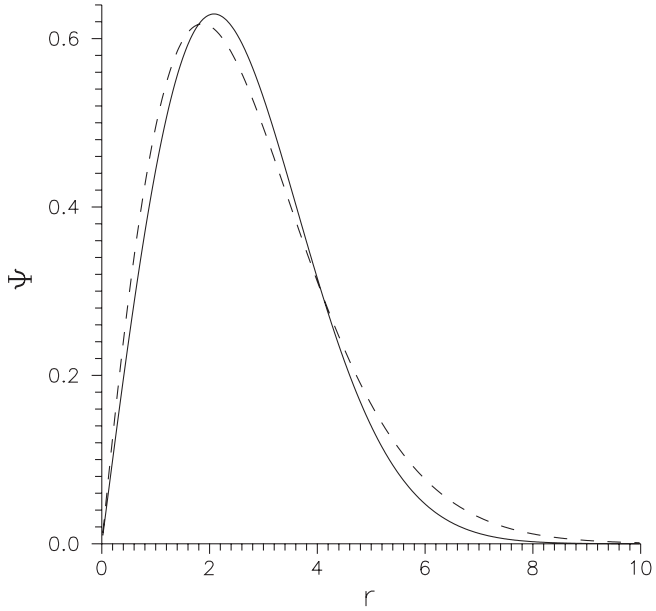


FIG. 4. The same as in Fig. 2, but for the $B$ meson with $k_{\max} = 1$.

In a similar way one calculates $J^{(1)}$, $J^{(2)}$,

$$J^{(1)}_{n,11}(\mathbf{p}, \mathbf{k}) = e^{-(\mathbf{p}^2/\Delta)-(\mathbf{k}^2/4\beta_2^2)} I_{n,11}(\mathbf{p}) \bar{y}^{(\pi)}_{123} \tag{21}$$

$$J^{(2)}_{n,11}(\mathbf{p}, \mathbf{k}_1, \mathbf{k}_2) = e^{-(\mathbf{p}^2/\Delta)-(\mathbf{K}^2/4\beta_2^2)(1)} I_{n,11}(\mathbf{p}) \tilde{y}^{(\pi\pi)}_{123} p_i. \tag{22}$$

In (22) we take into account that $\bar{y}^{(\pi\pi)}_{123}$ contains $q_i$ and $p_i$ and therefore the result of integration, over $d^3q$ leads to the modification of $I_{n,11}(\mathbf{p}) \equiv {}^{(0)}I_{n,11}(\mathbf{p})$, $I_{n,11}(\mathbf{p}) \to {}^{(1)}I_{n,11}(\mathbf{p})$. All these expressions are given in Appendix A.

Finally the matrix element $\mathcal{M}$ in (18) can be rewritten as

$$\mathcal{M} = \exp\left(-\frac{\mathbf{k}_1^2 + \mathbf{k}_2^2}{4\beta_2^2}\right)\left(\frac{M_{\rm br}}{f_\pi}\right)^2 \mathcal{M}_1 - \exp\left(-\frac{\mathbf{K}^2}{4\beta_2^2}\right)\frac{M_{\rm br} M_\omega}{f_\pi^2}\mathcal{M}_2 \tag{23}$$

and $\mathcal{M}_1$, $\mathcal{M}_2$ are given by the expressions

$$\mathcal{M}_1 = (Z_1^*)^2[{}^{(0)}\mathcal{L}^*_{nn'}(\omega_1) + {}^{(0)}\mathcal{L}^*_{nn'}(\omega_2)] + (Z_1^{**})^2[{}^{(0)}\mathcal{L}^{**}_{nn'}(\omega_1) + {}^{(0)}\mathcal{L}^{**}_{nn'}(\omega_2)]; \tag{24}$$

$$\mathcal{M}_2 = Z_2^2[{}^{(1)}\mathcal{L}^*_{nn'}(0) + {}^{(1)}\mathcal{L}_{nn'}(\omega_1 + \omega_2)] + (Z_2^*)^2[{}^{(1)}\mathcal{L}^*_{nn'}(0) + {}^{(1)}\mathcal{L}^*_{nn'}(\omega_1 + \omega_2)] + (Z_2^{**})^2[{}^{(1)}\mathcal{L}^{**}_{nn'}(0) + {}^{(1)}\mathcal{L}^{**}_{nn'}(\omega_1 + \omega_2)]. \tag{25}$$

Here ${}^{(k)}\mathcal{L}^s_{nn'}$ is the integral as in (13), and $s = (), *, **$ marks three channels: $B\bar{B}$, $B\bar{B}^* + \text{cc}$; $B^*\bar{B}^*$ respectively; $k = 0, 1$. The exact form for $\mathcal{L}$ is

$$ {}^{(k)}\mathcal{L}^{s}_{nn'}(\omega) = \int \frac{d^3\mathbf{p}}{(2\pi)^3} e^{-(\mathbf{p}^2/\beta_0^2)} \frac{{}^{(k)}I_{n,11}(p)^{(k)}I_{n',11}(p)(\frac{p}{\beta_0})^{2k}}{\frac{p^2}{2m_{BB}} - (\Delta M^{(s)} - \omega)} = \upsilon \int_0^\infty \frac{t^{k+(1/2)} dt e^{-t(k)} I_{n,11}(\sqrt{t}\beta_0)^{(k)}I_{n',11}(\sqrt{t}\beta_0)}{t - t^{(s)}(\omega)}. \quad (26) $$

Here $\upsilon$, $\beta_0$, $t^{(s)}(\omega)$ and $\Delta M^{(s)}$ are given in Appendix B.

Coefficients $Z_1^{(s)}$ and $Z_2^{(s)}$ define the relative weight of channels $s = B\bar{B}$, $B\bar{B}^*$ + c.c., $B^*\bar{B}^*$ with account of spin and isospin; it coincides with the corresponding coefficients found in Table IV of [35]. We obtain

$$ (Z_1^*)^2 = (Z_1^{**})^2 \cong 1, \qquad (Z_2^{**})^2 = 7Z_2^2, $$
$$ (Z_2^*)2 = 4Z_2^2, \qquad Z_2^2 = \frac{\beta_0^2}{6\omega^2}. \quad (27) $$

Now we can compute from ${}^{(1)}I_{n,11}$ the decay width of the $\Upsilon(nS)$ into $B\bar{B}$, $B\bar{B}^*$ + c.c., $B^*\bar{B}^*$, etc.

From (12), taking into account that $J_{nn_2n_3}(\mathbf{p}) = e^{-(\mathbf{p}^2/\Delta)(1)}I_{n,n_2n_3}(\mathbf{p})\frac{p_i}{\omega}$, and $\langle p_i p_k\rangle = \frac{1}{3}\delta_{ik}\mathbf{p}^2$, one obtains

$$ \Gamma(\Upsilon(nS) \to (B\bar{B})^{(s)}) = \left(\frac{M_\omega}{2\omega}\right)^2 \frac{M_B^{(s)} p_s^3}{6\pi N_c}(Z^{(s)})^2 \times e^{-(2\mathbf{p}_s^2/\Delta)}({}^{(1)}I_{n,n_2n_3}(p_s))^2 \quad (28) $$

where the channel index $s = ()$ for $B\bar{B}$, $M_B^{(*)} = \frac{2M_BM_B^*}{M_B+M_B^*}$ and for the $s = **$, decay channel is $B^*\bar{B}^*$, $M_B^{(**)} = M_B^*$, $(Z^{()})^2 = 1 (Z^{(*)}) = 4$, $(Z^{(**)})^2 = 7$.

## IV. THE ADLER-ZERO IMPROVEMENT OF MATRIX ELEMENTS

As was discussed in detail in [31] the general two-pion amplitude, consisting of one-pion vertices as in $\mathcal{M}_1$ and the two-pion vertex in $\mathcal{M}_2$, satisfies the Adler zero requirement, i.e., vanishes for $\mathbf{k}_i = \omega_i = 0$, if these amplitudes are imbedded in the general background not distinguishing one- and two- pion vertices. In particular, this implies summing up all closed channels of the type $B\bar{B}$. In [31] the AZI was realized representing the amplitude $\mathcal{M}$ in Eq. (23) in the form

$$ \mathcal{M} = \exp\left(-\frac{\mathbf{k}_1^2 + \mathbf{k}_2^2}{4\beta_2^2}\right)a(\omega_1, \omega_2) - \exp\left(-\frac{\mathbf{K}^2}{4\beta_2^2}\right)b(\omega_1, \omega_2) \quad (29) $$
$$ a = \left(\frac{M_{\rm br}}{f_\pi}\right)^2 \mathcal{M}_1, \qquad b = \frac{M_{\rm br}M_\omega}{f_\pi^2}\mathcal{M}_2 $$

and requiring that $a(\omega_1 = 0, \omega_2) = b(\omega_1 = 0; \omega_2)$, and the same for vanishing $k_2 = \omega_2 = 0$.

We shall now apply the AZI procedure to our decays under consideration, $n > n'$, $n = 4, 3, 2$. Before doing that, we introduce convenient new and universal variable $x$, which is in the interval [0,1] for all transitions.

$$ x = \frac{q^2 - 4m_\pi^2}{\mu^2}, \qquad \mu^2 = (\Delta E)^2 - 4m_\pi^2. \quad (30) $$

In terms of variables $x$, $\cos\theta$ the dipion decay probability can be written as

$$ dw_{\pi\pi}(n, n') = C_0\mu^3 \int_0^1 \sqrt{\frac{x(1-x)}{x + \frac{4m_\pi^2}{\mu^2}}} dx \frac{d\cos\theta}{2} \times |\mathcal{M}(x, \cos\theta)|^2. \quad (31) $$

Here $C_0 = \frac{1}{32\pi^3N_c^2} = 1.12 \cdot 10^{-4}$. Writing two exponents in (29) in terms of $x$, $\cos\theta$, one has (cf. Eq. (90) of [31])

$$ \mathbf{k}_1^2 + \mathbf{k}_2^2 \equiv \alpha + \gamma\cos^2\theta = \frac{\mu^2}{2}\left(1 - \frac{\Delta E}{M}(1-x) + \frac{x(1-x)}{x + \frac{4m_\pi^2}{\mu^2}}\cos^2\theta\right) \quad (32) $$

$$ \mathbf{K}^2 = \mu^2(1-x)(1-\delta) = \mu^2(1-x)\left(1 - \frac{\Delta E}{M}\right). \quad (33) $$

As it was found in [31], the AZI amplitude (29) vanishes for some value $x = \eta$, depending on the channel $(n, n')$ and this value of $\eta$ was calculated in [31]. Below we shall use these values and similarly to [31] represent the amplitude $\mathcal{M}(x, \cos\theta)$ as follows:

$$ \mathcal{M}(x, \cos\theta) = \mathcal{M}(x = \eta, \cos\theta) + \mathcal{M}'(x = \eta, \cos\theta)(x - \eta) + \ldots. \quad (34) $$

Here the prime denotes the derivative in $x$. It is important to note, that as explicit calculations show (see below), both $a$ and $b$ in (29) do not depend appreciably on $x$, and all $x$ dependence in $\mathcal{M}$ is coming from the exponential factors. Using (32) and (33), one arrives at the following representation for $\mathcal{M}$,

$$ \mathcal{M}(x, \cos\theta) = \mathcal{M}_1(\eta, \cos\theta)\left(\frac{M_{\rm br}}{f_\pi}\right)^2 \times \frac{\mu^2}{4\beta_2^2} e^{-(\bar{\alpha} + \bar{\gamma}\cos^2\theta/4\beta_2^2)}(x - \eta)f(\eta), \quad (35) $$

where $\bar{\alpha} = \alpha(x = \eta)$, $\bar{\gamma} = \gamma(x = \eta)$ and $f(\eta)$ appears due to derivatives in $x$ of (32) and (33)

$$ f(x) = 1 + \frac{\Delta E}{2M} - \cos^2\theta \frac{x^2 + (1-2x)\frac{4m_\pi^2}{\mu^2}}{2(x + \frac{4m_\pi^2}{\mu^2})^2}. \quad (36) $$

Thus all calculations of the dipion spectra in the AZI scheme reduce to the calculation of $\mathcal{M}_1$ given in Eq. (24),

TABLE I. Parameters of $(n, n')$ transitions and resulting widths $\Gamma_{\pi\pi}(n, n')$ in comparison with $\Gamma_{\rm exp}$ taken from [36].

| $(n, n')$ | 2,1 | 3,1 | 3,2 | 4,1 | 4,2 |
|---|---|---|---|---|---|
| $\mu$, GeV | 0.483 | 0.85 | 0.174 | 1.083 | 0.479 |
| $\mu^2$, GeV$^2$ | 0.234 | 0.721 | 0.03 | 1.172 | 0.229 |
| $\mathcal{M}_1$, GeV$^{-1}$ | −1.56 | 0.592 | −1.66 | −0.452 | 0.688 |
| $\mathcal{M}_2$, GeV$^{-1}$ | −0.122 | −0.116 | −0.322 | −0.0199 | −0.354 |
| $\eta$ | 0 | 0.56 | −2.7 | 0.3 | 0.61 |
| $\Gamma/(\frac{M_{br}}{f_\pi})^4$ (keV) | 0.132 | 0.195 | 0.311 | 0.552 | 0.0071 |
| $\Gamma_{\rm exp}$ (keV) | 6 | 0.56 | 0.9 | <2 | <6 |

at some intermediate point $x = \eta$, and subsequent integrations as in Eq. (31). The values of $\mu$ and $\eta$ for all transitions are given in Tables I and II.

This procedure refers to all $(n, n')$ transitions of our set, except for the (3,2) transition. In the latter case the value of $\eta = \eta_{\rm AZI}$ found in [31] is large and negative, $\eta \cong -3$ and expansion (34) does not make sense for $x$ in the physical interval [0,1]. Therefore one can instead explicitly compute $\mathcal{M}_1$ and $\mathcal{M}_2$ in (23) as given by (24) and (25) and insert $M_\omega = \sqrt{2}\omega \approx 0.8$ GeV (to be checked below by pionless decays). Computed in this way amplitudes $\mathcal{M}_1$, $\mathcal{M}_2$, $\eta$ and resulting values of $\Gamma_{\pi\pi}^{(n,n')} = \int dw_{\pi\pi}(n, n')$ are given in the Table I.

We turn now to the dipion spectra as functions of $x$ and $\cos\theta$. For the AZI decay amplitudes for the processes $(n, n') = (2, 1), (3, 1), (4, 1), (4, 2)$ one can use the form (36); however for the 2d plots in $x$, $\cos\theta$ one should take into account that $\eta$ depends on $\cos\theta$. Indeed, in the general AZI form of the dipion decays' amplitude (30) one can see that the first exponent on the right-hand side depends on $\cos\theta$ (cf. Eq. (33)), hence vanishing of $\mathcal{M}$ occurs at some $x = \tilde{\eta}(cos\theta)$, where

$$\tilde{\eta}(\cos\theta) = \eta - \gamma\cos^2\theta = \eta - \frac{1}{2}\frac{(1-\eta)\eta\cos^2\theta}{\eta + \frac{4m_\pi^2}{\mu^2}}. \quad (37)$$

Correspondingly, one should replace in (36) $\eta$ by $\tilde{\eta}$ given in (37), however this amounts to a small correction for all four transitions under investigation.

The amplitude $\mathcal{M}(x, \cos\theta)$ can be expanded in a complete set of polynomials in the region $0 \le x \le 1$, $-1 \le \cos\theta \le 1$. One can write for this purpose a product of orthonormal polynomials $\bar{p}_n(x)p_l(z)$, where $\bar{p}_n(x) = \sqrt{2n+1}P_n(2x-1)$, $p_l(z) = \sqrt{\frac{2l+1}{2}}P_l(z)$, and $P_k(u)$ is the Legendre polynomial, so that

$$\frac{dw}{dq d\cos\theta} = \mu^2 C_0\sqrt{x(1-x)}|\mathcal{M}|^2 = \sum_{n,l=0}^{\infty} a_{nl}\bar{p}_n(x)p_l(\cos\theta) \quad (38)$$

$$a_{nl} = \int_0^1 dx \int_{-1}^{+1} dz \frac{dw}{dq d\cos\theta}\bar{p}_n(x)p_l(z). \quad (39)$$

Tables III, IV, V, VI, and VII of coefficients $a_{nl}$ for our $\mathcal{M}(x, \cos\theta)$ computed according to Eq. (39) with $\eta \to \tilde{\eta}$ are given in Appendix B.

## V. RESULTS AND DISCUSSION

Let us reiterate the approximations and assumptions made in the derivation of our formalism. We note that pions can be emitted by heavy quarkonia only from internal light quark loops, which immediately implies that the intermediate states directly produced by (1) and (3) can be only $B\bar{B}$, $B_s\bar{B}_s$ or their excitations. We introduced two $q\bar{q}$ vertices with or without accompanying pions and take minimal number of vertices for each process, since additional vertices yield a small correction, e.g., creating $q\bar{q}\pi$ first by the $q\bar{q}$ vertex $M_\omega$ and then creating the pion due to the $B^* \to B\pi$ vertex with the width $\Gamma_\pi$ yields a correction $O(\Gamma_\pi/\omega) \ll 1$; an additional $\pi\pi\bar{q}q$ vertex yields the cor-

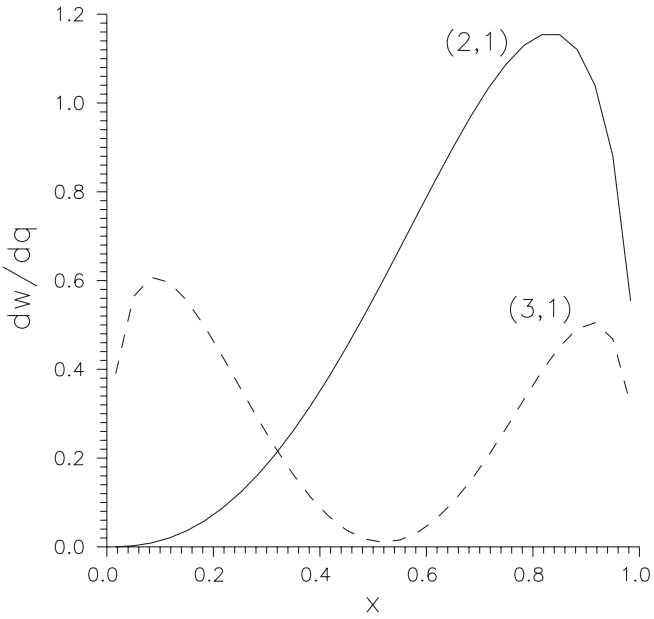


FIG. 5. Dipion spectrum $\frac{dw}{dq}$ as a function of $x$ for (2,1) and (3,1) transitions.

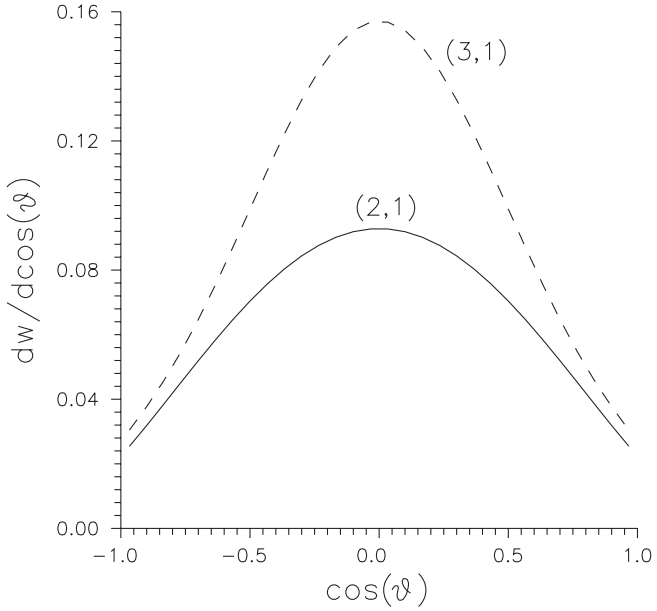


FIG. 6. Dipion spectrum $\frac{dw}{dq}$ as a function of cos$\theta$ for the (2,1) and (3,1) transitions.

rection $M_{\rm br}/\omega \ll 1$. Starting from (1) and (3), one can derive effective vertices $\Upsilon^*\Upsilon(\rho, \omega)$, etc. We have not considered those leaving it for future development. Finally, we have retained the lowest states $B\bar{B}$, $B\bar{B}^*$ + c.c., $B^*\bar{B}^*$ and neglect higher excitations. We expect that inclusion of higher excited states yields renormalization of our vertices $M_{\rm br}$ and $M_\omega$, which are only fitting parameters, the same for all processes. For the shape of the spectra the crucial point is the relative renormalization of amplitudes $a$ and $b$ in (29) and this is fixed by the AZI procedure. As will be seen from our results, our theoretical predictions are in reasonable agreement with experiment.

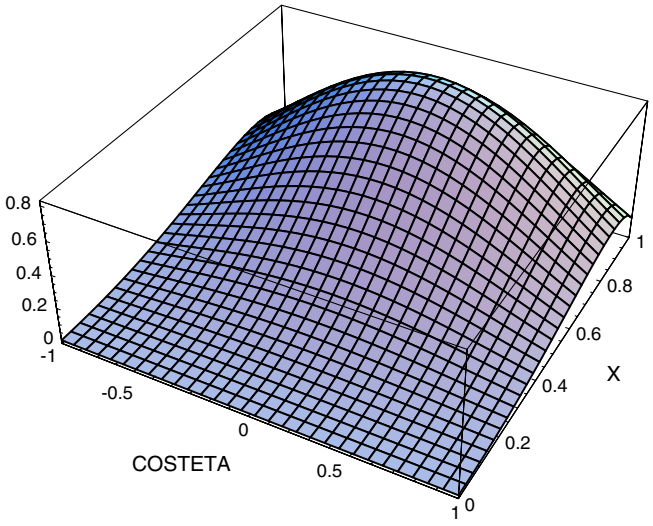


FIG. 7 (color online). The 2$d$ dipion spectrum $\frac{d^2w(2,1)}{dqd\cos\theta}$ as a function of $x$, cos$\theta$ for the (21) transition.

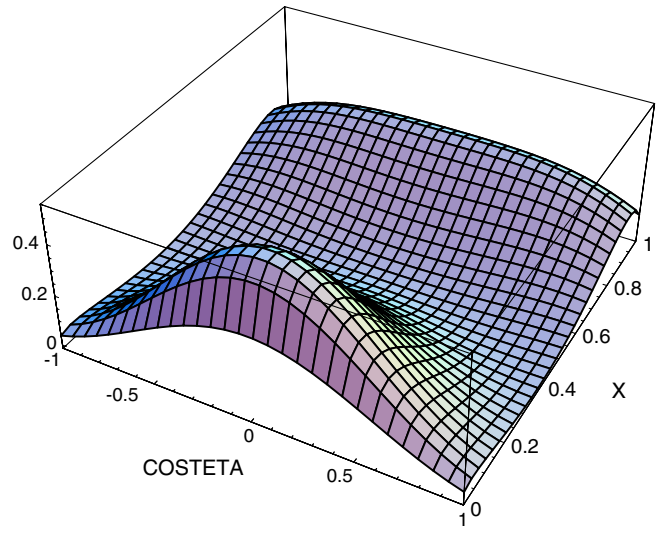


FIG. 8 (color online). The same as in Fig. 7, but for the (3,1) transition.

We start with the $B\bar{B}$ widths, which define our only input parameters $M_{\rm br}$ and $M_\omega$. As shown in (30), for the $\Upsilon(4S) \to B\bar{B}$ decay one can write

$$\Gamma_{4S}(B\bar{B}) = \left(\frac{M_\omega}{2\omega}\right)^2 0.0033 |J^{(4)}_{BB}(p)|^2 \text{ GeV} \qquad (40)$$

where $J^{(4)}_{BB}(p) = \exp(-\frac{p^2}{\Delta})^{(1)} I_{411}(p)$, and $\Delta = 2\beta_1^2 + \beta_2^2$ and the overlap integral $I_{411}$ is known from the wave functions of $\Upsilon(4S)$ and $B$ meson, which are fitted by oscillator functions with $\beta_1$ and $\beta_2$ respectively. Here

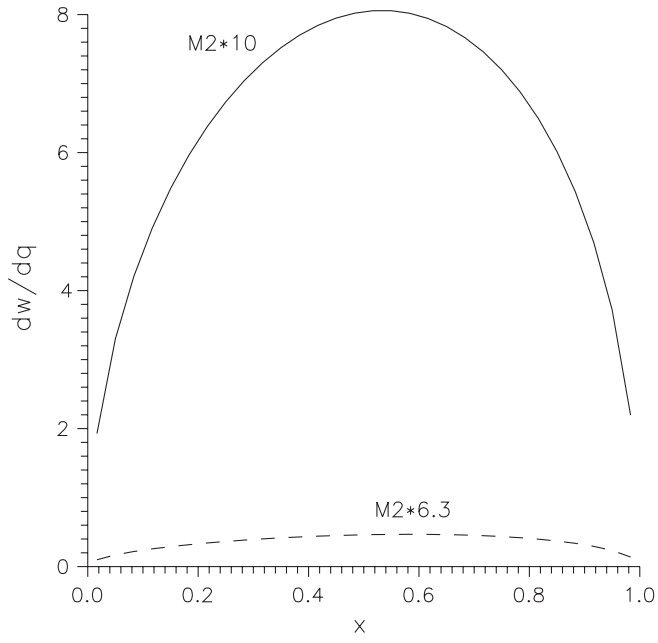


FIG. 9. The same as in Fig. 5, but for the (3,2) transition. Numbers on the curves (6,3) and (10) refer to the value of ratio $\frac{M_\omega}{M_{br}}$ used in Eq. (18).

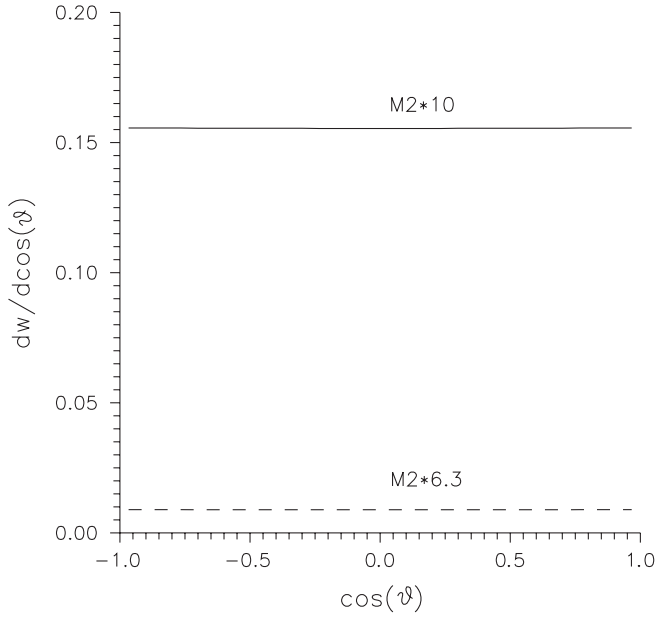


FIG. 10. The same as in Fig. 9, but for $\frac{dw}{d\cos\theta}$ the (3,2) transition.

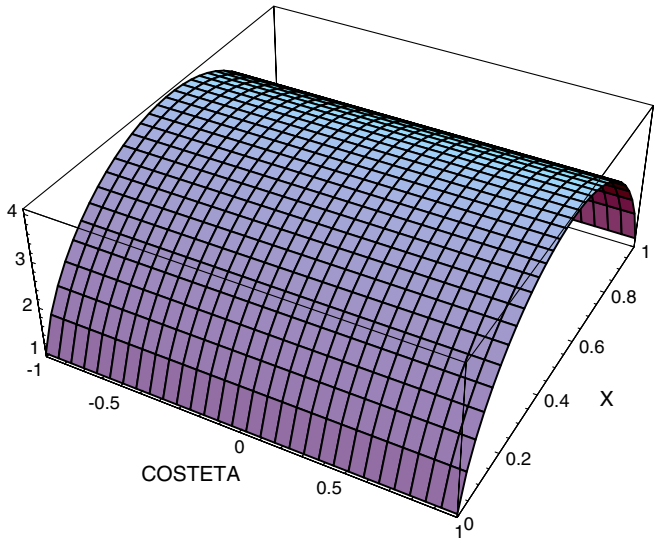


FIG. 11 (color online). The same as in Fig. 7, but for the (3,2) transition and $\frac{M_\omega}{M_{br}} = 10$.

$p = 0.33$ GeV is the $B$ meson momentum. Approximating the $\Upsilon(4S)$ wave function with 4 and 15 oscillator functions one obtains $J^{(4)}_{B\bar{B}}(0.33) = -0.8434$ and $-3.63$ respectively, which yields $\frac{\Gamma_{4S}(B\bar{B})}{(\frac{M_\omega}{2\omega})^2} = 2.4$ MeV and 44 MeV.

This sensitivity of $\Gamma_{4S}$ to the wave functions is typical for all results of total width, both with pion emission and without. One can exploit this fact and invert the procedure to find the $S$ wave function (e.g., position of zeros) from the values of widths.[2] As it is, we consider the 15-term approximation for the $\Upsilon(4S)$ wave function good enough (see Fig. 3 for comparison) and can define $M_\omega$ comparing $\Gamma_{\text{theor}}$ with $\Gamma_{\text{exp}}(\Upsilon(4S) \to B\bar{B}) = (20.5 \pm 2.5)$ MeV [36], which yields $\frac{M_\omega}{2\omega} \simeq 0.68$ or $M_\omega \approx 0.8$ GeV with an accuracy of $\pm 10\%$. However, the accuracy of the wave function calculation in [33] and its simulation by oscillator functions is not well known, and to be on the safe side, we conclude that $M_\omega \approx 2\omega$ as an order of magnitude estimate. We now turn to the total dipion widths $\Gamma_{\pi\pi}(nn')$ given in Table I.

[2]The authors are grateful to M. V. Danilov for this suggestion

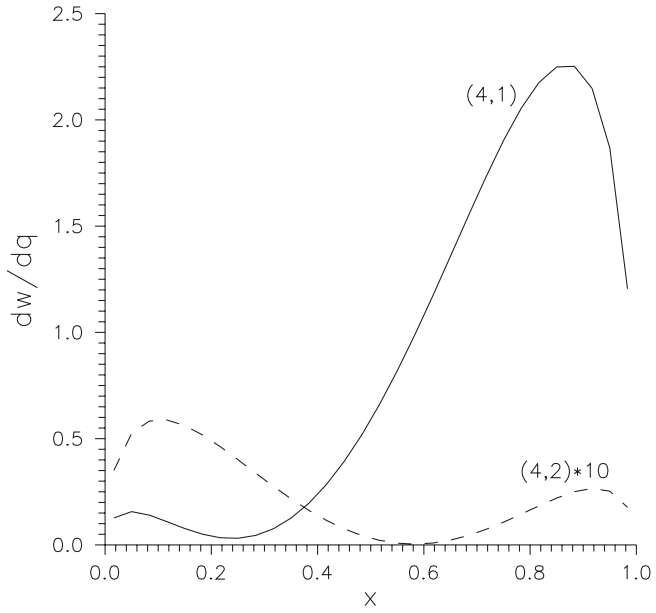


FIG. 12. The same as in Fig. 5, but for the (4,1) and (4,2) transitions.

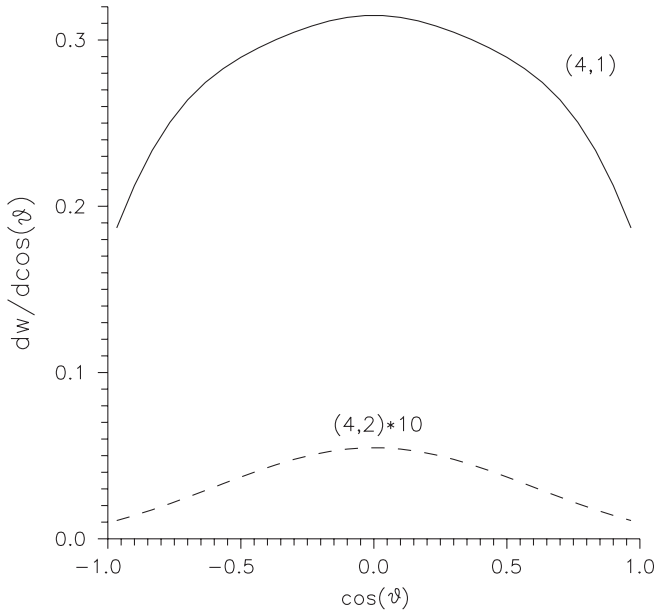


FIG. 13. The same as in Fig. 6, but for the (4,1) and (4,2) transitions.

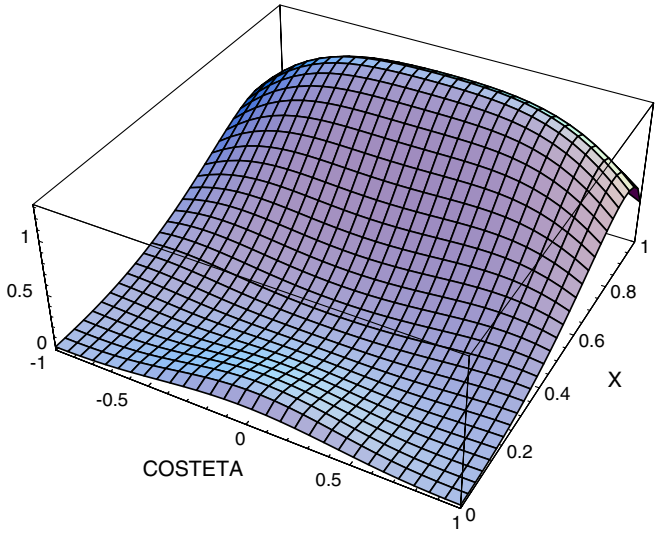


FIG. 14 (color online). The same as in Fig. 7, but for the (4,1) transition.

Comparing two last lines in the table for $\Gamma_{\rm theor}$ and $\Gamma_{\rm exp}$ one can see that one gets a correct order of magnitude for $\frac{\Gamma_{\rm theor}}{(\frac{M_{br}}{f_\pi})^4}$, so that the factor $(\frac{M_{\rm br}}{f_\pi})^4$ can be taken in the interval $1 \le (\frac{M_{\rm br}}{f_\pi})^4 \le 6$, i.e., $1 \le \frac{M_{\rm br}}{f_\pi} \le 1.45$. A large discrepancy for $\Gamma(21)$ in Table I possibly is due to poor approximation of the $\Upsilon(2S)$ wave function.

In this way we are supporting our assumption that string decay with and without pion emission is governed by two different scale parameters, $M_{\rm br}$ and $M_\omega$, which differ by 1 order of magnitude, $M_\omega \approx (6 \div 10)M_{\rm br}$. Moreover each of the parameters is defined by its dynamical mechanism: $M_\omega \approx 2\omega$ due to time-turning trajectories, and $M_{\rm br} \sim f_\pi$ due to chiral decay Lagrangian.

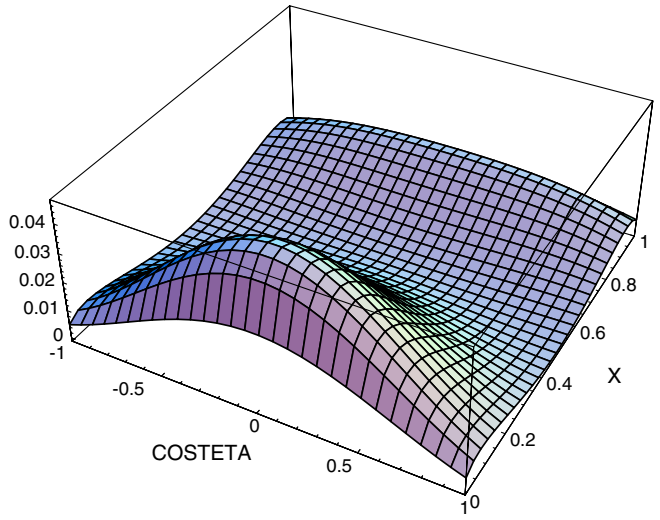


FIG. 15 (color online). The same as in Fig. 7, but for the (4,2) transition.

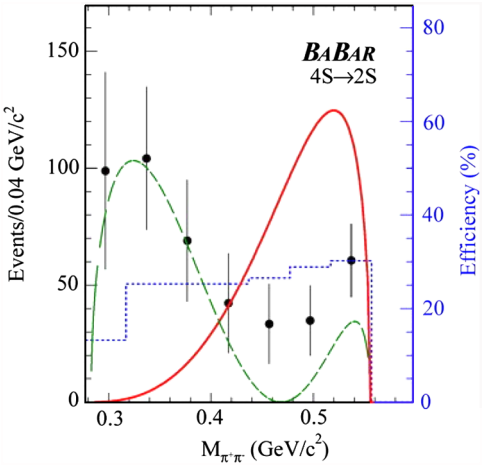


FIG. 16 (color online). Comparison of data from [6] with parametrization (35) (broken line).

Now we turn to the dipion spectra. For each transition $(nn')$ we show in Figs. 5–15 three spectra: $\frac{dw}{dq}$, $\frac{dw}{d\cos\theta}$ and $\frac{d^2w}{dqd\cos\theta}$, where the 1d spectra are integrated over another variable. For comparison the existing experimental spectra are given in Figs. 16–18, taken from [6–8] with theoretical curves from [31,32] where $\eta$ is independent of $\cos\theta$.

One can see a general qualitative and semiquantitative agreement between theoretical and experimental spectra. One should stress again that while the total dipion width is sensitive to the form of wave functions, the qualitative form of the spectrum is defined by the value of $\eta \approx \tilde{\eta}$, which accumulates the information on overlap matrix elements and stabilized when the AZI condition is imposed. The case of the (3.2) transition has a special feature of low available phase space, and therefore the spectrum as function of $x$ is defined mostly by the phase space factor

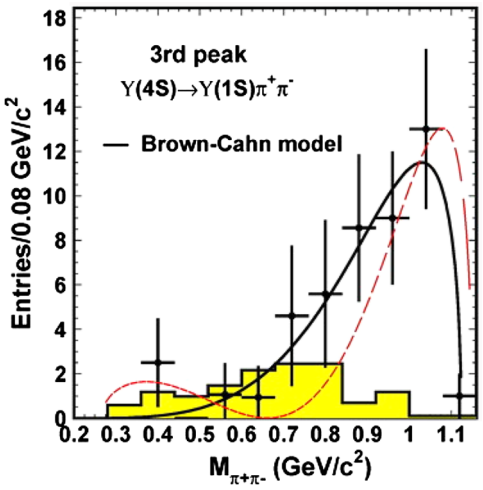


FIG. 17 (color online). Comparison of data from [8] with parametrization (35) (broken line).

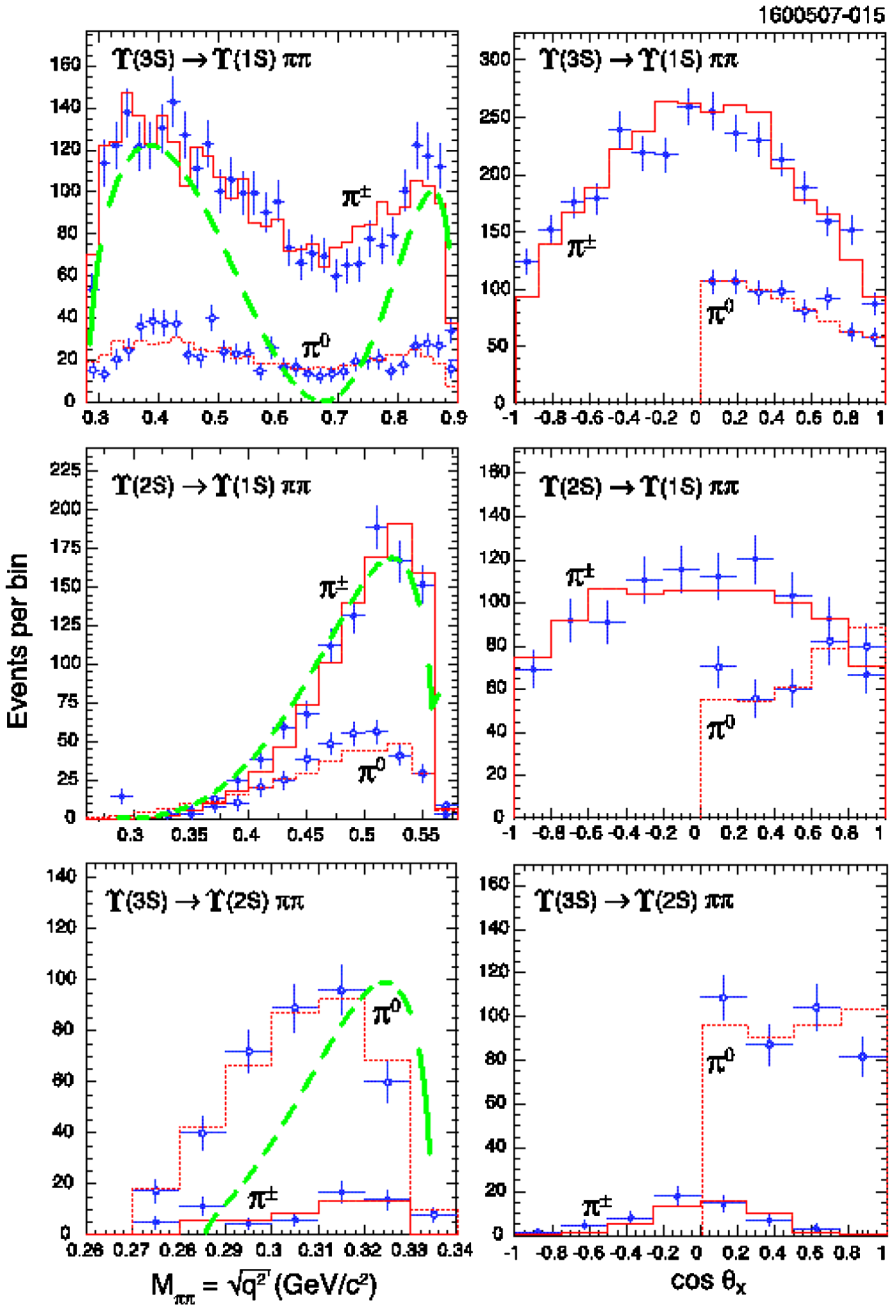


FIG. 18 (color online). Comparison of data from [6] with parametrization (35) and parameter $\eta$ from Table I (dashed line) (from [31].

$[x(1-x)]^{1/2}$, while dependence on $\cos\theta$ is also weak due to small $\mu^2 = 0.03$ GeV$^2$.

Thus all features of spectra and total widths can be understood in terms of the formalism, presented in [31,32] and in this paper above. Note, that our more refined analysis in the present paper has required two important changes as compared with the formalism in [31,32]. First, two independent decay scales $M_{\rm br}$ and $M_\omega$ are introduced and estimated here in contrast to the only parameter $M_{\rm br}$ in [31,32]. Second, the correction was introduced in the $P$-wave vertex, viz. $\bar{y}_{123}$ in Eq. (7), which decreases the effective value of this vertex. However, in the AZI form the $P$-wave vertices (the amplitude $\mathcal{M}_2$ in (23)) are derived from the Adler zero condition, as in (29) and (35), and the resulting form of the total AZI amplitude is the same as in [31,32] (with additional weak $\cos\theta$ dependence in $\tilde{\eta}(\cos\theta)$ neglected there).

## VI. CONCLUSIONS AND OUTLOOK

We have derived the amplitudes, spectra and total widths of dipion emission in all subthreshold processes $\Upsilon(nS) \to \Upsilon(n'S)\pi\pi$, with $n = 2, 3, 4$ and $n' = 1, 2$. We have shown that the formalism of pair creation, based on two effective Lagrangians, CDL and RDL with two mass parameters, $M_{\rm br}$ and $M_\omega$ respectively, can successfully describe the experimentally found spectra. Moreover, it was shown that two distinct values of widths, $\Gamma_{nS}(B\bar{B}) = O(10\ \text{MeV})$ and $\Gamma_{\pi\pi}(nn') = O(1\ \text{keV})$, can be explained by much different scales of $M_\omega \approx 2\omega = 0(1\ \text{GeV})$ and $M_{\rm br} \approx f_\pi = 0(100\ \text{MeV})$. Fixing in this way $M_\omega$ and $M_{\rm br}$ one obtains parameter-free one- and two-dimensional spectra in good qualitative and semiquantitative agreement with experimental data.

The application of this formalism to the case of $\Upsilon(5S)$ states and dipion transitions to $\Upsilon(2S)$, $\Upsilon(1S)$ is straightforward and is also successful [37]. The main difference is that the $5S$ state is above the $BB$, $BB^*$ + c.c., $B^*B^*$ thresholds and hence the amplitudes $\mathcal{M}_1$, $\mathcal{M}_2$ acquire large imaginary parts, which strongly deform the spectra and are affected by final state $\pi\pi$ interaction.

Another direct application of the formalism to the one-pion or $\eta$ transitions is clearly visible and is done in [38].

## ACKNOWLEDGMENTS

The authors are grateful to many useful remarks and suggestions of participants of seminars at ITEP (Moscow) and ITP (Heidelberg). Support and suggestions of M. V. Danilov and S. I. Eidelman are gratefully acknowledged. Data, advice and help from A. M. Badalian and B. L. G. Bakker were very important for the authors. This work was financially supported by the grants RFFI 06-02-17012 and NSh-4961.2008.2, and also grant RFFI 06-02-17120.

## APPENDIX A: CALCULATION OF THE COEFFICIENT $\bar{y}_{123}$ IN EQ. (5)

General formalism for the calculation of the overlap matrix elements and, in particular, of the factor $\bar{y}_{123}$ in (5) is given in Appendix 1 of [31]. Here we present the corrected form, where all relative momenta are properly defined. One starts with the calculation of the trace, Eq. (6), which gives (cf. Eq. (52) of [31]).

$$\bar{Z} = \frac{im_Q}{2\Omega\omega}\left(p_{qi} - p_{\bar{q}i} + \frac{\omega}{2\Omega}(P_{Q_i} - P_{\bar{Q}i}) + O\left(\frac{1}{\Omega^2}\right)\right). \tag{A1}$$

For the $(Q\bar{q})$) system one can define total and relative momenta as

$$\mathbf{P}_1 = \mathbf{p}_Q + \mathbf{p}_{\bar{q}}, \qquad \mathbf{q}_1 = \frac{\omega_{\bar{q}}\mathbf{p}_Q - \Omega_Q\mathbf{p}_{\bar{q}}}{\omega_{\bar{q}} + \Omega_Q} \tag{A2}$$

and the same for the $(\bar{Q}q)$ system.

$$\mathbf{P}_2 = \mathbf{p}_{\bar{Q}} + \mathbf{p}_q, \qquad \mathbf{q}_2 = \frac{\omega_q\mathbf{p}_{\bar{Q}} - \Omega_{\bar{Q}}\mathbf{p}_q}{\omega_q + \Omega_{\bar{Q}}}. \tag{A3}$$

In the total c.m. system $\mathbf{P}_1 = \mathbf{p}$, $\mathbf{P}_2 = -\mathbf{p}$ and

$$\mathbf{p}_{\bar{q}} = -\mathbf{q}_1 + \frac{\omega}{\omega + \Omega}\mathbf{p} \tag{A4}$$

$$\mathbf{p}_q = -\mathbf{q}_2 - \frac{\omega}{\omega + \Omega}\mathbf{p}; \qquad \mathbf{p}_Q = \mathbf{p} - \mathbf{p}_{\bar{q}}; \qquad \mathbf{p}_{\bar{Q}} = -\mathbf{p} - \mathbf{p}_q. \tag{A5}$$

Finally one obtains from (A1), taking into account that $\mathbf{q}_2 = -\mathbf{q}_1 \equiv -\mathbf{q}$,

$$\bar{y}_{123} \approx \bar{Z}_i = \frac{im_Q}{2\Omega^2\omega}\left[q_i(2\Omega + \omega) - p_i\frac{\omega\Omega}{\omega + \Omega}\right]. \tag{A6}$$

The appearance of the term $O(q_i)$ in (A6) leads to the change of the result of integration over $d^3\mathbf{q}$ in Eq. (5) as compared to the standard integral ${}^{(0)}I_{n,11}(p)$, given in (A16). Separating the factor $\frac{p_i}{\omega}$, one arrives at the expression

$$\begin{aligned} {}^{(1)}J_{n,11}(\mathbf{p}) &= \int \bar{y}_{123}(p,q)\frac{d^3q}{(2\pi)^3}\psi(nS, \mathbf{q} + \mathbf{p})\psi^2_{\rm HL}(\mathbf{q}) \\ &= \frac{ip_i}{\omega}\sum_k c_k^{(n)}a_k\left(-\frac{2}{\Omega + \omega}\left(\frac{\omega}{2} + \Omega\frac{\beta_2^2}{\Delta_n}\right)\right. \\ &\quad \left. + \frac{8\beta_1^2\beta_2^2\partial}{\Delta_n^2 y\partial f^2}\right)\Phi\left(-(k-1), \frac{3}{2}, f^2\right). \end{aligned} \tag{A7}$$

Here $a_k$, $\beta_1$, $\beta_2$, $\Delta_n$, $y$ are defined in Appendix B, and $c_k^{(n)}$ are coefficients of expansion of $\psi(nS, \mathbf{q})$ over oscillator functions (see Appendix B for more details).

The SHO basis functions $\{\varphi_k(\beta r)\}$ can be written as

$$\varphi_k(\beta, r) = c_k\frac{H_{2k-1}(\beta r)}{\beta r}e^{-((\beta r)^2/2)}. \tag{A8}$$

With the normalization condition $\int \varphi_k(z)\varphi_{k'}(z)d^3z = \delta_{kk'}$ and coefficients

$$c_k = \frac{1}{(2^{2k}\pi^{3/2}(2k-1)!)^{1/2}}. \tag{A9}$$

One can write Hermite polynomials in (A8) as

$$\frac{H_{2n-1}(x)}{x} = (-1)^{n-1}2\frac{(2n-1)!}{(n-1)!}\Phi\left(-(n-1), \frac{3}{2}, x^2\right) \tag{A10}$$

where

$$\Phi(\alpha, \gamma, x^2) = 1 + \frac{\alpha}{\gamma}\frac{x^2}{1!} + \frac{\alpha(\alpha+1)}{\gamma(\gamma+1)}\frac{(x^2)^2}{2!} + \ldots. \tag{A11}$$

Any radial excited state $nS$, $n = 1, 2, 3, \ldots$ can be expanded as

$$\psi(nS;\beta,r)=\sum_{k=1}^{\infty}c_k^{(n)}\varphi_k(\beta r); \tag{A12}$$

the overlap matrix element can be written as

$$J_{n;1,1}(p)\equiv\int\frac{d^3q}{(2\pi)^3}\psi(nS;\mathbf{q}+\mathbf{p})\psi^2_{\mathrm{HL}}(1S;\mathbf{q}) \tag{A13}$$

where the heavy-light meson wave function is

$$\psi_{\mathrm{HL}}(n'S;\beta_2,r)=\sum_k\bar{c}_k^{(n')}\varphi_k(\beta_2,r) \tag{A14}$$

$$J_{n;1,1}(\mathbf{p})=\sum_{k(k_1,k_2)}c_k^{(n)}\bar{c}_{k_1}^{(1)}\bar{c}_{k_2}^{(1)}\int\frac{d^3q}{(2\pi)^3}\varphi_k(\beta_1,\mathbf{q}+\mathbf{p})\times\varphi_{k_1}(\beta_2,\mathbf{q})\varphi_{k_2}(\beta_2,\mathbf{q}) \tag{A15}$$

$$\int\frac{d^3q}{(2\pi)^3}\varphi_n(\beta_1,\mathbf{q}+\mathbf{p})\varphi_1(\beta_2,\mathbf{q})\varphi_1(\beta_2,\mathbf{q})=e^{-(\mathbf{p}^2/\Delta)(0)}I_{n,1,1}(\mathbf{p})=e^{-(\mathbf{p}^2/\Delta)}\tilde{c}_n(-1)^{n-1}2\frac{(2n-1)!}{(n-1)!}\times\Phi\left(-(n-1),\frac{3}{2},f^2\right)\frac{y^{n-1}}{(2\sqrt{\pi})^3}\left(\frac{2\beta_1^2\beta_2^2}{\Delta_n}\right)^{3/2}, \tag{A16}$$

where

$$\Delta_n=2\beta_1^2+\beta_2^2,\qquad y=\frac{2\beta_1^2-\beta_2^2}{2\beta_1^2+\beta_2^2},\qquad\mathbf{f}=\frac{2\mathbf{p}\beta_1}{\Delta_n\sqrt{y}};$$
$$\tilde{c}_n=\left(\frac{2\pi}{\beta_1}\right)^{3/2}\frac{(2\sqrt{\pi}/\beta_2)^3}{(2^{2n}\pi^{3/2}(2n-1)!)^{1/2}}$$

## APPENDIX B: COEFFICIENTS OF THE OVERLAP INTEGRALS $^{(k)}\mathcal{L}^{(s)}_{nn'}(\omega)$

For the given intermediate state $s=(),*,**$ thresholds $E_s$ are $2M_B$, $M_B+M_{B^*}$, $2M_{B^*}$ respectively, and one can define $\Delta M^{(s)}=E_s-M$, where $M$ is the mass of $\Upsilon(nS)$. The resulting values of $\Delta M^{(s)}_{nn'}$ are given below in Table II. We also assemble here some formulas for the quantities appearing in Eqs. (25) and (26). Namely,

$$\upsilon\equiv\frac{2\tilde{M}^{(s)}\beta_0}{(2\pi)^2},\qquad\beta_0^2=\frac{\Delta_n\Delta_{n'}}{\Delta_n+\Delta_{n'}},$$
$$\Delta_n=2\beta_1^2+\beta_2^2,\qquad\Delta_{n'}=2(\beta_1')^2+\beta_2^2, \tag{B1}$$

where $\beta_1$, $\beta_1'$ are oscillator parameters found from the fitting of realistic $(nS)$, $(n'S)$ wave functions with a series of oscillator wave functions. Both $\beta_1$ and $\beta_1'$ depend on the number $k_{\max}$ of functions kept in the series.

$$\tilde{M}^{(s)}=\frac{1}{2}M_B,\quad\frac{M_BM_{B^*}}{M_B+M_{B^*}},\quad\frac{1}{2}M_B^*\quad\text{for } s=(),*,**, \tag{B2}$$

$$t^{(s)}(\omega)=\frac{2\tilde{M}^{(s)}}{\beta_0^2}(\Delta M^{(s)}-\omega),\qquad s=(),*,**. \tag{B3}$$

Other useful relations are

$$k_1^2+k_2^2=\alpha+\gamma\cos^2\theta=\frac{\mu^2}{2}\left(1-\frac{\Delta E}{M}(1-x)+\frac{x(1-x)}{x+\frac{0.08}{\mu^2}}\cos^2\theta\right) \tag{B4}$$

$$(\mathbf{k}_1+\mathbf{k}_2)^2=\mu^2(1-x)\left(1-\frac{\Delta E}{M}\right) \tag{B5}$$

$$\omega_{1,2}=\frac{\Delta E}{2}-\frac{\mu^2(1-x)}{4M}\mp\frac{\mu}{2}\left(1-\frac{\Delta E}{2M}\right)\times\left(\frac{x(1-x)}{x+\frac{0.08}{\mu^2}}\right)^{1/2}\cos\theta. \tag{B6}$$

## APPENDIX C: COEFFICIENTS OF THE 2D EXPANSION OF THE PROBABILITY

As is given in (38) and (39), the full probability $\frac{dw}{dqd\cos\theta}$ can be expanded in products of polynomials

$$\frac{dw}{dqd\cos\theta}=\sum_{n,l=0}^{n_{\max},l_{\max}}a_{ln}\bar{p}_n(x)p_l(\cos\theta) \tag{C1}$$

with

TABLE II. Values of the mass parameter in (23)–(26).

| $(n/n')$ | 21 | 31 | 32 | 41 | 42 |
|---|---|---|---|---|---|
| $\mu$ (GeV) | 0.483 | 0.85 | 0.174 | 1.083 | 0.479 |
| $\mu^2$ GeV$^2$ | 0234 | 0.721 | 0.03 | 1.172 | 0.229 |
| $\Delta E$, GeV | 0.56 | 0.895 | 0.332 | 1.12 | 0.556 |
| $\Delta M_{nn'}$ GeV | −0.54 | −0.205 | −0.205 | 0.02 | 0.02 |
| $\Delta M^{*}_{nn'}$ GeV | −0.58 | −0.25 | −0.25 | −0.026 | −0.026 |
| $\Delta M^{**}_{nn'}$ GeV | −0.625 | −0.295 | −0.295 | −0.072 | −0.072 |

TABLE III. The coefficients $a_{ln}$ defined as in (C1) for the transition (2,1).

| $n$ / $l$ | 0 | 1 | 2 | 3 | 4 |
|---|---|---|---|---|---|
| 0 | 0.3890825 | 0.2707011 | −0.0407149 | −0.0996852 | −0.0427755 |
| 2 | −0.1300538 | −0.0895548 | 0.0148794 | 0.0335517 | 0.0138329 |
| 4 | 0.0109938 | 0.0072973 | −0.0016296 | −0.0029011 | −0.0010309 |

TABLE IV. The same as in Table III for the transition (3,1).

| $n$ / $l$ | 0 | 1 | 2 | 3 | 4 |
|---|---|---|---|---|---|
| 0 | 0.2054341 | −0.0268913 | 0.1136786 | 0.0082049 | −0.0731623 |
| 2 | −0.0739902 | 0.0651164 | −0.0402644 | −0.0209861 | 0.0284658 |
| 4 | 0.0145838 | −0.0245765 | 0.0033265 | 0.0089023 | −0.0048144 |

TABLE V. The same as in Table III for the transition (3,2).

| $n$ / $l$ | 0 | 1 | 2 | 3 | 4 |
|---|---|---|---|---|---|
| 0 | 4.4761992 | 0.1298668 | −1.2300728 | −0.0479114 | −0.1895183 |
| 2 | −0.0037809 | −0.0002265 | 0.0005379 | 0.0001151 | 0.0003569 |
| 4 | −0.0248627 | −0.0007194 | 0.0068405 | 0.0002649 | 0.0010495 |

TABLE VI. The same as in Table III for the transition (4,1).

| $n$ / $l$ | 0 | 1 | 2 | 3 | 4 |
|---|---|---|---|---|---|
| 0 | 0.6245209 | 0.5257702 | 0.0810291 | −0.1920402 | −0.1252025 |
| 2 | −0.0786476 | −0.0707901 | −0.0530417 | 0.0376144 | 0.0335737 |
| 4 | −0.0212058 | −0.0278274 | 0.0141198 | 0.0064219 | −0.0028386 |

TABLE VII. The same as in Table III for the transition (4,2).

| $n$ / $l$ | 0 | 1 | 2 | 3 | 4 |
|---|---|---|---|---|---|
| 0 | 0.0165037 | −0.0083040 | 0.0080081 | 0.0029911 | −0.0055958 |
| 2 | −0.0063807 | 0.0055190 | −0.0024492 | −0.0020172 | 0.0019898 |
| 4 | 0.0010072 | −0.0012899 | 0.0000858 | 0.0004939 | −0.0002193 |

$$\bar{p}_n(x) = \sqrt{2n+1}P_n(2x-1), \qquad p_l(z) = \sqrt{\frac{2l+1}{2}}P_l(z). \tag{C2}$$

The coefficients $a_{nl}$ calculated for $\frac{dw}{dqd\cos\theta}$ in (38), for transitions $(n, n') = (2, 1), (3, 1), (4, 1), (4, 2)$ are given below together with $a_{nl}$ for the (3,2) transition, calculated as in (23). Note that $a_{ln} \equiv 0$ for odd $l$.

[1] T. M. Himel Ph.D. thesis, Stanford University [Institution Report No. SLAC-223, 1979)]; M. Oreglia (Crystal Ball Collaboration), Phys. Rev. Lett. **45**, 959 (1980); H. Albrecht (ARGUS Collaboration), Z. Phys. C **35**, 283 (1987); J. Z. Bai (BES Collaboration), Phys. Rev. D **62**, 032002 (2000).
[2] F. Butler *et al.* (CLEO Collaboration),Phys. Rev. D **49**, 40 (1994).
[3] S. Glenn *et al.* (CLEO Collaboration), Phys. Rev. D **59**, 052003 (1999).
[4] J. P. Alexander *et al.* (CLEO Collaboration), Phys. Rev. D **58**, 052004 (1998).
[5] I. C. Brock*et al.* (CLEO Collaboration), Phys. Rev. Daz **43**, 1448 (1991).
[6] B. Aubert *et al.* (*BABAR* Collaboration), Phys. Rev. Lett. **96**, 232001 (2006).
[7] K. Abe *et al.*, (BELLE Collaboration), Phys. Rev. D **75**, 071103 (2007).
[8] D. Cronin-Hennessy *et al.* (CLEO Collab.), Phys. Rev. D **76**, 072001 (2007).
[9] L. S. Brown and R. N. Cahn, Phys. Rev. Lett. **35**, 1 (1975).
[10] M. B. Voloshin, Pis'ma Zh. Eksp. Teor. Fiz. **21**, 733 (1975) [JETP Lett. **21**, 347 (1975)].
[11] K. Gottfried, Phys. Rev. Lett. **40**, 598 (1978).
[12] T. M. Yan, Phys. Rev. D **22**, 1652 (1980).
[13] M. B. Voloshin and V. I. Zakharov, Phys. Rev. Lett. **45**, 688 (1980); V. A. Novikov and M. A. Shifman, Z. Phys. C **8**, 43 (1981).
[14] H.-W. Ke, Jian Tang, X.-Q. Hao, and X.-Q. Li, Phys. Rev. D **76**, 074035 (2007).
[15] G. Belanger, T. De Grand, and P. Moxhay, Phys. Rev. D **39**, 257 (1989).
[16] S. Chakravarty, S. M. Kim, and P. Ko, Phys. Rev. D **50**, 389 (1994).
[17] T. Komada, S. Ishida, and M. Ishida, Phys. Lett. B **508**, 31 (2001); **518**, 47 (2001).
[18] M. Uehara, Prog. Theor. Phys. **109**, 265 (2003).
[19] M. B. Voloshin, Pis'ma Zh. Eksp. Teor. Fiz **37**, 58 (1983) [JETP Lett. **37**, 69 (1983)].
[20] V. V. Anisovich, D. V. Bugg, A. V. Sarantsev, and B. S. Zhou, Phys. Rev. D **51**, R4619 (1995).
[21] F.-K. Guo, P.-N. Shen, H.-C. Chiang, and R.-G. Ping, Nucl. Phys. **A761**, 269 (2005).
[22] H. J. Lipkin and S. F. Tuan, Phys. Lett. B **206**, 349 (1988).
[23] H.-Y. Zhou and Y-P. Kuang, Phys. Rev. D **44**, 756 (1991).
[24] M. B. Voloshin, Phys. Rev. D **74**, 054022 (2006).
[25] S. Chakravarty, S. M. Kim, and P. Ko, Phys. Rev. D **48**, 1212 (1993).
[26] P. Moxhay, Phys. Rev. D **39**, 3497 (1989).
[27] F.-K. Guo, P.-N. Shen, H.-C. Chiang, and R.-G. Ping, Phys. Lett. B **658**, 27 (2007).
[28] Ce Meng and K.-T. Chao, Phys. Rev. D **77**, 074003 (2008).
[29] H. G. Dosch, Phys. Lett. B **190**, 177 (1987); H. G. Dosch and Yu. A. Simonov, Phys. Lett. B **205**, 339 (1988); Yu. A. Simonov, Nucl. Phys. **B307**, 512 (1988); A. Di. Giacomo, H. G. Dosch, V. I. Shevchenko, and Yu. A. Simonov, Phys. Rep. **372**, 319 (2002); arXiv:hep-ph/0007223.
[30] Yu. A. Simonov, Phys. Rev. D **65**, 094018 (2002).
[31] Yu. A. Simonov, Phys. At. Nucl. **71**, 1048 (2008).
[32] Yu. A. Simonov, JETP Lett. **87**, 21 (2008).
[33] A. M. Badalian, A. I. Veselov, and B. L. G. Bakker, J. Phys. G **31**, 417 (2005); Phys. At. Nucl. **70**, 1764 (2007).
[34] S. Weinberg, Phys. Rev. Lett. **67**, 3473 (1991); J. L. Goity and W. Roberts, Phys. Rev. D **60**, 034001 (1999).
[35] Yu. S. Kalashnikova, Phys. Rev. D **72**, 034010 (2005).
[36] W.-M. Yao *et al.* (Particle Data Group), J. Phys. G **32**, 1 (2006).
[37] Yu. A. Simonov and A. I. Veselov, arXiv:0805.4499; Phys. Lett. B **671**, 55 (2009).
[38] Yu. A. Simonov and A. I. Veselov, arXiv:0806.2919; arXiv:0810.0366.